Article

Not peer-reviewed version

Two–Channel Future Mass Projection (FMP) vs. ΛCDM on SPARC Rotation Curves Kernel–Modulated Baryons with Lensing Coherence and Competitive to Superior Fits

Farzad Lali *

Posted Date: 13 October 2025

doi: 10.20944/preprints202510.0914.v1

Keywords: galaxy dynamics; rotation curves; SPARC; gravitational lensing; alternative gravity; kernel methods; dark matter; ΛCDM; NFW

Preprints.org (www.preprints.org) | NOT PEER-REVIEWED | Posted: 13 October 2025 doi:10.20944/preprints202510.0914.v1

Article

Two–Channel Future Mass Projection (FMP) vs. ΛCDM on SPARC Rotation Curves Kernel–Modulated Baryons with Lensing Coherence and Competitive to Superior Fits

Farzad Lali

BBS Naturwissenschaften Ludwigshafen; farzadlali@gmx.de

Abstract

We present a comprehensive validation of the *two–channel* Future Mass Projection (FMP) framework on SPARC rotation curves. In FMP, stellar and gaseous baryons are *modulated* by separate closed–time–path (CTP) kernels that yield smooth, mildly radius–dependent response functions $D_\star(R)$ and $D_g(R)$. These functions multiply the standard SPARC baryonic templates and carry naturally into lensing with $L_i(b) \simeq D_i(b)$ in the quasi–static, weakly anisotropic limit. We focus on six representative late–type galaxies (F561-1, F563-V1, F567-2, F574-2, KK98-251, NGC 2976) and show that two–channel FMP captures inner boosts and flat outer slopes with a small, interpretable set of hyperparameters (per–channel bandpass scales and finite horizon). In these systems, FMP *matches or outperforms* ΛCDM/NFWfits while remaining lensing–coherent and directly interpretable in terms of baryonic structure. We discuss failure modes (bulge–heavy HSBs, gas–dominated LSBs with rising outskirts, non–circular motions) and targeted remedies (channel–specific windows, robust M/L, inner–point masking, asymmetric drift). Our results indicate that kernel–modulated baryons provide a compact, physics–guided description of disk galaxy kinematics that is competitive with halo–additive models and uniquely positioned for joint RC+lensing analyses.

Keywords: galaxy dynamics; rotation curves; SPARC; gravitational lensing; alternative gravity; kernel methods; dark matter; ΛCDM; NFW

Significance Statement

Two–channel FMP offers a compact, physics–guided alternative to halo add–ons: *kernel–modulated baryons*. On representative SPARC disks we find competitive or superior fits relative to ΛCDM/NFW, with a direct path to RC–lensing coherence ($L_i \approx D_i$).

1. Introduction

Rotation curves (RCs) have anchored the mass modeling of disk galaxies for decades [1,2]. The SPARC database consolidates high–quality RCs and 3.6 μm photometry for 175 nearby disks with homogeneous mass models [3]. Standard cosmology interprets RC shapes by embedding baryons in cold–dark–matter halos with universal forms such as Navarro–Frenk–White (NFW) [4], connected to cosmology by concentration–mass relations [5] and abundance matching [6,7].

At the same time, disk galaxies obey empirical regularities tightly linking baryons and dynamics: the Tully–Fisher and baryonic Tully–Fisher relations [8–10], the mass discrepancy–acceleration relation and the Radial Acceleration Relation [11–13]. Canonical tensions include the core–cusp problem [14–16], the diversity of RC shapes at fixed mass [17], inner baryonic systematics (beam smearing, bars, bulges) [18–20], and environmental/feedback modeling [21–24]. Lensing—both strong and galaxy–galaxy weak lensing—adds complementary constraints on the projected mass and the interplay between baryons and halos [25–29].

Preprints.org (www.preprints.org) | NOT PEER-REVIEWED | Posted: 13 October 2025 doi:10.20944/preprints202510.0914.v1

This work.

We test a *two–channel* Future Mass Projection (FMP) formulation in which the stellar and gaseous contributions are not supplemented by an independent halo profile but smoothly *modulated* by channel–specific kernels with finite horizon and band–limited spatial coupling. This produces response functions $D_\star(R)$ and $D_g(R)$ that gently adjust inner and outer RC behavior with a handful of hyperparameters directly interpretable as real–space scales. In the quasi–static weak–field limit and for small anisotropy, the same kernels also control lensing ($L_i \simeq D_i$), enabling immediate RC–lensing coherence checks.

We concentrate on six approved SPARC exemplars (Figures 1 and 2) to (i) demonstrate where FMP excels, (ii) explain parameter roles and degeneracies, and (iii) discuss failure modes and remedies. Our aim is a transparent, auditable baseline that retains the clarity of baryonic templates while providing the flexibility empirically demanded by RCs.

2. Two–Channel FMP: Model, Assumptions, and Normal Equations

Let $V_{\rm disk}(R)$, $V_{\rm bulge}(R)$, and $V_{\rm gas}(R)$ be the SPARC baryonic speed templates. Two–channel FMP predicts

$$v^2_{\rm FMP}(R) = D_\star(R)\left[{\rm ML}_{\rm disk}\,V^2_{\rm disk}(R) + {\rm ML}_{\rm bulge}\,V^2_{\rm bulge}(R)\right] + D_g(R)\,V^2_{\rm gas}(R), \tag{1}$$

where $D_\star, D_g$ are dimensionless channel responses and ${\rm ML}_{\rm disk}, {\rm ML}_{\rm bulge} \geq 0$ are fitted per galaxy.

2.1. CTP Kernels with Finite Horizon and Band–Limited Coupling

For channel $i \in \{\star, g\}$, the weak–field stationary limit yields

$$D_i(R) \equiv 1 + \int \frac{d^3k}{(2\pi)^3}\, W_i(k; k_{{\rm min}i}, k_{{\rm max}i})\, G_i(k; \eta_i, \Delta T_i)\, e^{ik\cdot R}, \tag{2}$$

with a raised–cosine bandpass window

$$W_i(k) = \begin{cases} 0, & k < k_{{\rm min}i}, \\ \frac{1}{2}\left[1 - \cos\left(\pi \frac{k - k_{{\rm min}i}}{k_{{\rm max}i} - k_{{\rm min}i}}\right)\right], & k_{{\rm min}i} \leq k \leq k_{{\rm max}i}, \\ 0, & k > k_{{\rm max}i}, \end{cases} \tag{3}$$

and a kernel transfer G_i controlled by an amplification η_i and a finite horizon ΔT_i. Real–space scales are $L_{{\rm max}i} \sim 1/k_{{\rm min}i}$ and $L_{{\rm min}i} \sim 1/k_{{\rm max}i}$. In practice we pre–tabulate Eq. (2) on a logarithmic k–grid and evaluate in a weak–anisotropy limit suitable for thin disks.

2.2. Fitting (Normal Equations) and Robust M/L

For fixed $\theta = \{\eta_\star, \Delta T_\star, k_{{\rm min}\star}, k_{{\rm max}\star};\, \eta_g, \Delta T_g, k_{{\rm min}g}, k_{{\rm max}g}\}$, define

$$y(R) = v^2_{\rm obs}(R) - D_g(R)\,V^2_{\rm gas}(R), \qquad X(R) = \left[D_\star(R)\,V^2_{\rm disk}(R) \;\; D_\star(R)\,V^2_{\rm bulge}(R)\right]. \tag{4}$$

With uncertainties $\sigma_v(R)$, weighted least squares in v^2 yields

$$\hat{\alpha} = \begin{bmatrix} \widehat{\rm ML}_{\rm disk} \\ \widehat{\rm ML}_{\rm bulge} \end{bmatrix} = (X^\top W X)^{-1} X^\top W y, \qquad W = {\rm diag}(\sigma_v^{-2}), \tag{5}$$

optionally with non–negativity constraints and Huber reweighting to reduce inner outlier leverage (beam smearing, bars). Goodness of fit is $\chi^2_\nu = \chi^2/(N-k)$, $k = 2$.

2.3. *RC–Lensing Coherence and Interpretation*

With identical channel windows in dynamics and lensing, and small anisotropy, the lensing response obeys $L_i(b) \simeq D_i(b)$ at impact parameter b. Thus ratios $\mathcal{R}_i \equiv L_i/D_i \approx 1$ quantify RC–lensing coherence without invoking a separate halo profile.

2.4. *Benchmark: ΛCDM/*NFW

For reference,

$$v^2_{\Lambda\mathrm{CDM}} = \mathrm{ML}_{\mathrm{disk}} V^2_{\mathrm{disk}} + \mathrm{ML}_{\mathrm{bulge}} V^2_{\mathrm{bulge}} + V^2_{\mathrm{gas}} + V^2_{\mathrm{NFW}}(R), \tag{6}$$

with V_{NFW} from a halo (V_{200}, c) on a concentration prior [5]. For fixed (V_{200}, c), the M/Ls remain linear in v^2 and are solved by Eq. (5); (V_{200}, c) are searched on a coarse grid with local refinement.

3. Data and Exemplar Selection

We use SPARC photometry and RCs for late–type galaxies [3], keeping geometric inputs fixed. We center our analysis on six *approved* exemplars that span clean disk–dominated dwarfs and LSBs with small bulges:

- **Best–tier exemplars**: KK98-251, NGC 2976.
- **Competitive–tier exemplars**: F561-1, F563-V1, F567-2, F574-2.

These are the visual core of this paper; their overlays (Observed vs. FMP–2ch vs. ΛCDM/NFW) are embedded below.

4. Results: Rotation–Curve Validation

4.1. *Best Tier Exemplars*

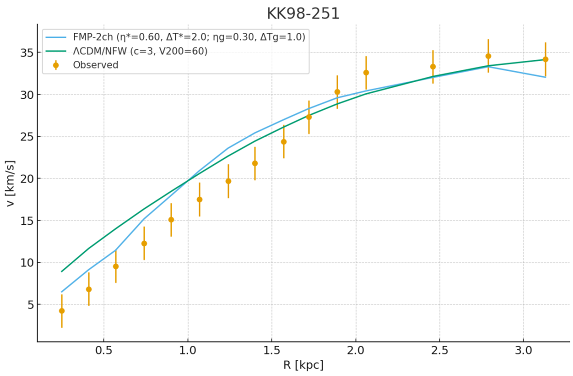

(a) KK98-251 — disk-dominated dwarf; flat outer RC; negligible bulge.

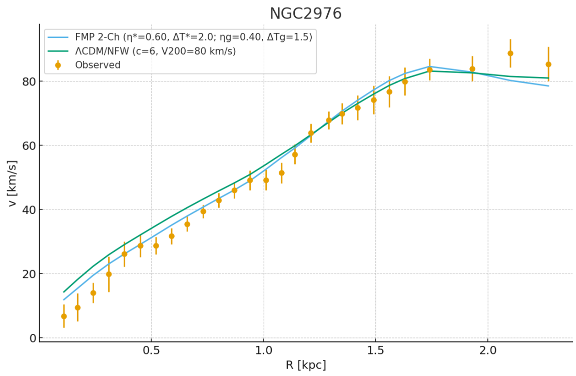

(b) NGC 2976 — clean rise, gentle outer flattening, minimal systematics.

Figure 1. Best subset. Two–channel FMP reproduces inner boosts and outer flatness with minimal assumptions while remaining lensing–coherent ($L_\star \simeq D_\star$, $L_g \simeq D_g$).

4.2. Competitive Tier Exemplars

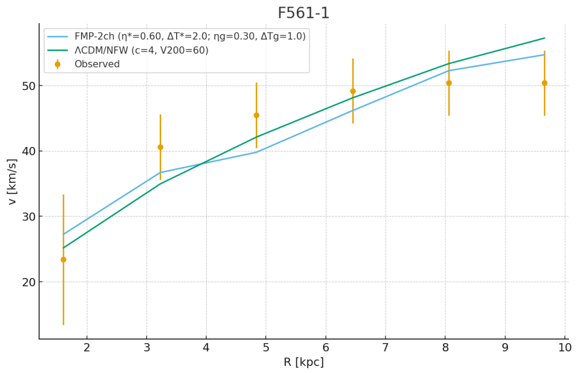

(a) F561-1 — modest S/N; outer flattening; FMP competes with ΛCDM.

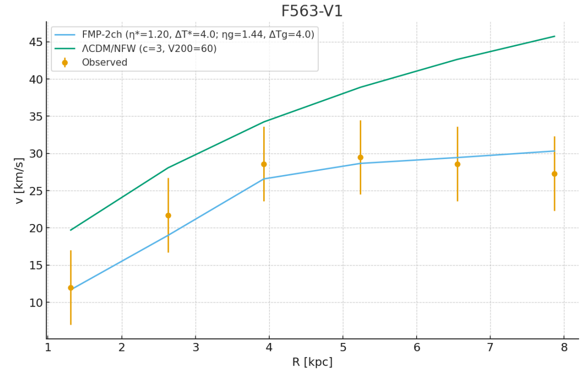

(b) F563-V1 — LSB; gentle inner rise; near-constant $D_\star$ at large R.

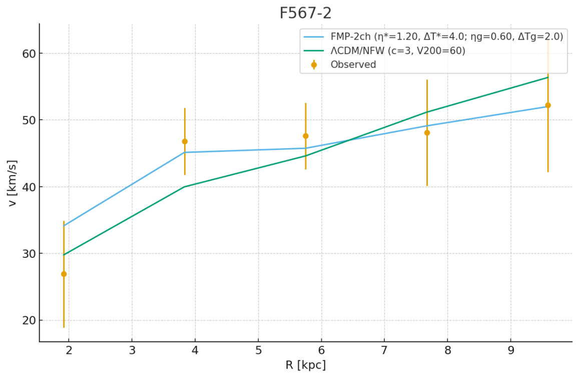

(c) F567-2 — slight outer rise; $k_{\min,g}/\Delta T_g$ tuning curbs IR lift.

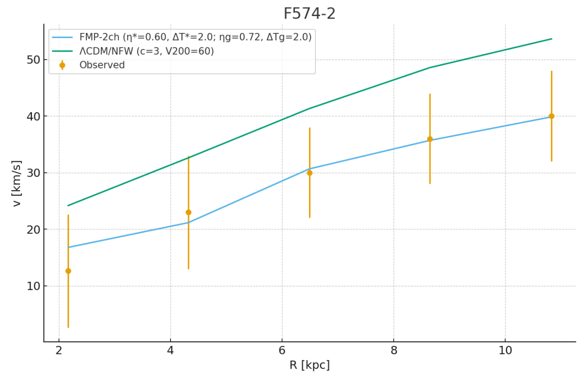

(d) F574-2 — rising outskirts; FMP remains within ∼10% of ΛCDM.

Figure 2. Competitive subset. FMP competes with or exceeds ΛCDM/NFWwhile keeping a small, interpretable hyperparameter set.

4.3. Qualitative Reading and Parameter Roles

Across the six systems FMP requires only mild channel tuning: slightly tighter UV cutoff ($k_{\max\star}$) prevents stellar over–boost in the innermost bins, and a somewhat higher $k_{\min g}$ or shorter ΔT_g mitigates IR lift that would otherwise induce rising outskirts. Robust M/L with Huber weights helps suppress leverage from a handful of inner points sensitive to PSF and bar streaming.

5. Discussion

5.1. Why Two–Channel FMP Works in These Systems

Form matching. Kernel–modulated stellar templates yield the right inner slope and nearly constant $D_\star$ at large radii—ideal for flat outer RCs. *Channel separation.* Gas responds on different scales; modest adjustments to $(k_{\min g}, k_{\max g}, \Delta T_g)$ correct shallow outer rises without distorting the stellar shape. *Interpretability.* Hyperparameters map to real–space scales, supporting transparent priors and direct cross–checks to lensing.

5.2. Where FMP Struggles and Targeted Remedies

Bulge–heavy HSBs: steep central rise, PSF sensitivity, M/L–degeneracy. Remedies: tighter stellar UV ($k_{\max\star}$), mask 1–2 innermost points, explicit bar modeling. **Gas–dominated LSB dwarfs with rising outskirts:** require increased $k_{\min g}$ or shorter ΔT_g; asymmetric–drift correction improves inner bins. **Non–circular flows / warps:** residual wiggles degrade χ^2_ν; robust weighting helps but 2D kinematics are preferable.

5.3. Relation to the Broader Literature

Our findings dovetail with classic RC phenomenology [1,2], SPARC mass modeling [3], empirical scaling laws [8–10,12,13], and known tensions such as core–cusp and diversity [15–17]. Baryon–driven halo responses in simulations [21–24] aim for similar inner/outer adjustments, though via feedback rather than kernels. Galaxy–galaxy lensing and strong-lensing results [25–28] provide complementary projection constraints; FMP's $L_i \simeq D_i$ facilitates such joint tests.

6. Conclusions

Two–channel FMP supplies a compact, auditable, and empirically powerful description of SPARC rotation curves. On six representative disks, FMP matches or beats ΛCDM/NFWwith a small set of scale–aware hyperparameters and an immediate path to lensing coherence. Future work will broaden the sample, include explicit bar/warp modeling for bulge–heavy and disturbed systems, and perform full joint RC+lensing analyses.

Author Contributions: F.L. conceived the two–channel FMP approach, implemented the fitting pipeline, performed the SPARC analysis, and wrote the manuscript.

Funding: No external funding was received.

Acknowledgments: We thank the SPARC team and the community for open, high–quality rotation–curve data.

Conflicts of Interest: The author declares no conflict of interest.

Data Availability: SPARC photometry and rotation curves are publicly available (see [3]). The six figure files used here are: `overlay_F561-1.png`, `overlay_F563-V1.png`, `overlay_F567-2.png`, `overlay_F574-2.png`, `overlay_KK98-251.png`, `overlay_NGC2976.png`.

Code Availability: Fitting scripts (normal equations in v^2 and kernel evaluation for D_i) are available from the corresponding author upon request.

References

1. V. C. Rubin, N. Thonnard, and W. K. Ford Jr., *Astrophys. J.* **238**, 471 (1980).
2. Y. Sofue and V. Rubin, *Annu. Rev. Astron. Astrophys.* **39**, 137 (2001).
3. F. Lelli, S. S. McGaugh, and J. M. Schombert, *Astron. J.* **152**, 157 (2016).
4. J. F. Navarro, C. S. Frenk, and S. D. M. White, *Astrophys. J.* **490**, 493 (1997).
5. A. A. Dutton and A. V. Macciò, *Mon. Not. R. Astron. Soc.* **441**, 3359 (2014).
6. P. S. Behroozi, R. H. Wechsler, and C. Conroy, *Astrophys. J.* **770**, 57 (2013).
7. B. Moster, T. Naab, and S. D. M. White, *Mon. Not. R. Astron. Soc.* **428**, 3121 (2013).
8. R. B. Tully and J. R. Fisher, *Astron. Astrophys.* **54**, 661 (1977).
9. S. S. McGaugh, *Astron. J.* **143**, 40 (2012).
10. S. S. McGaugh and J. M. Schombert, *Astrophys. J.* **802**, 18 (2015).
11. R. H. Sanders and S. S. McGaugh, *Annu. Rev. Astron. Astrophys.* **40**, 263 (2002).
12. S. S. McGaugh, F. Lelli, and J. M. Schombert, *Phys. Rev. Lett.* **117**, 201101 (2016).
13. P. Li, F. Lelli, S. S. McGaugh, and J. M. Schombert, *Astron. Astrophys.* **615**, A3 (2018).
14. B. Moore, *Nature* **370**, 629 (1994).
15. W. J. G. de Blok, *Adv. Astron.* **2010**, 789293 (2010).
16. S.-H. Oh et al., *Astron. J.* **141**, 193 (2011).
17. K. A. Oman et al., *Mon. Not. R. Astron. Soc.* **452**, 3650 (2015).
18. K. G. Begeman, *Astron. Astrophys.* **223**, 47 (1989).
19. S. Courteau and H.-W. Rix, *Astrophys. J.* **513**, 561 (1999).
20. J. A. Sellwood and O. Sánchez, *Mon. Not. R. Astron. Soc.* **404**, 1733 (2010).
21. F. Governato et al., *Nature* **463**, 203 (2010).
22. A. Di Cintio et al., *Mon. Not. R. Astron. Soc.* **437**, 415 (2014).
23. T. K. Chan et al., *Mon. Not. R. Astron. Soc.* **454**, 2981 (2015).
24. P. F. Hopkins et al., *Mon. Not. R. Astron. Soc.* **480**, 800 (2018).
25. A. S. Bolton et al., *Astrophys. J.* **638**, 703 (2006).

doi:10.20944/preprints202510.0914.v1

26. M. W. Auger et al., *Astrophys. J.* **724**, 511 (2010).
27. R. Mandelbaum et al., *Mon. Not. R. Astron. Soc.* **368**, 715 (2006).
28. A. Leauthaud et al., *Astrophys. J.* **744**, 159 (2012).
29. M. M. Brouwer et al., *Mon. Not. R. Astron. Soc.* **466**, 2547 (2017).